

Article

Investigation into the Effects of Citric Acid on the Corrosion Behavior of AM 350 Stainless Steel Using Electrochemical Impedance Spectroscopy

Citlalli Gaona-Tiburcio ¹, Miguel Villegas-Tovar ¹, Erick Maldonado-Bandala ^{2,*},
María Lara-Banda ¹, Miguel Angel Baltazar-Zamora ², Ce Tochtli Méndez-Ramírez ²,
Demetrio Nieves-Mendoza ², Verónica Almaguer-Cantu ³, Jesus Manuel Jaquez-Muñoz ⁴,
Aldo Landa-Gómez ² and Facundo Almeraya-Calderón ^{1,*}

¹ FIME, Centro de Investigación e Innovación en Ingeniería Aeronáutica (CIIA), Universidad Autónoma de Nuevo León, San Nicolás de los Garza 66455, Mexico; citlalli.gaonatbr@uanl.edu.mx (C.G.-T.); miguel.villegastvr@uanl.edu.mx (M.V.-T.); maria.laraba@uanl.edu.mx (M.L.-B.)

² Facultad de Ingeniería Civil, Universidad Veracruzana, Xalapa 91000, Mexico; mbaltazar@uv.mx (M.A.B.-Z.); cmendez@uv.mx (C.T.M.-R.); dneives@uv.mx (D.N.-M.); alandag@uv.mx (A.L.-G.)

³ Instituto de Biotecnología, Facultad de Ciencias Biológicas, Universidad Autónoma de Nuevo León, San Nicolás de los Garza 66455, Mexico; veronica.almaguerct@uanl.edu.mx

⁴ Instituto Tecnológico de Ciudad Juárez, Av. Tecnológico, 1340, Ciudad Juárez 32500, Mexico; jesus.jaquezmn@uanl.edu.mx

* Correspondence: erimaldonado@uv.mx (E.M.-B.); facundo.almerayacl@uanl.edu.mx (F.A.-C.)



Academic Editors: Marija B. Petrović Mihajlović, Ana Simonovic, Milan B. Radovanović and Žaklina Z. Tasić

Received: 12 March 2025

Revised: 1 April 2025

Accepted: 7 April 2025

Published: 8 April 2025

Citation: Gaona-Tiburcio, C.; Villegas-Tovar, M.; Maldonado-Bandala, E.; Lara-Banda, M.; Baltazar-Zamora, M.A.; Méndez-Ramírez, C.T.; Nieves-Mendoza, D.; Almaguer-Cantu, V.; Jaquez-Muñoz, J.M.; Landa-Gómez, A.; et al. Investigation into the Effects of Citric Acid on the Corrosion Behavior of AM 350 Stainless Steel Using Electrochemical Impedance Spectroscopy. *Metals* **2025**, *15*, 420. <https://doi.org/10.3390/met15040420>

Copyright: © 2025 by the authors. Licensee MDPI, Basel, Switzerland. This article is an open access article distributed under the terms and conditions of the Creative Commons Attribution (CC BY) license (<https://creativecommons.org/licenses/by/4.0/>).

Abstract: Stainless steels are used in the aeronautical industry for their corrosion resistance and good mechanical performance. The chemical treatment used to improve corrosion resistance is passivation, forming a compact, continuous, adherent chromium oxide film. This research aimed to investigate the effect of citric acid at different concentrations (citric acid; citric acid + oxalic acid, citric acid + hydrogen peroxide, and citric acid + hydrogen peroxide + ethanol) on AM 350 stainless steel passivated for 90 and 120 min at 25 and 50 °C and immersed in 5% by weight sodium chloride (NaCl) solutions. The electrochemical technique used was electrochemical impedance spectroscopy (EIS) based on ASTM-G106. The EIS (equivalent circuit) results indicate that there are one and two constant phase elements (CPE), which indicate the presence of various factors on the stainless steel surface, such as roughness and the formation of porous and passive layers, respectively. A double-layer system was employed for some samples. However, when the ethanol was added to the passivation bath, the behavior changed to a one-time constant system. The AM 350 passivated in citric and oxalic acid presented the higher corrosion resistance with values of $6 \times 10^5 \Omega \cdot \text{cm}^2$.

Keywords: corrosion; electrochemical impedance spectroscopy; stainless steels

1. Introduction

Due to its unique properties, stainless steel (SS) is essential in various industries. From construction to food, medical, automotive, and aerospace applications, it is indispensable for its durability, corrosion resistance, versatility, and esthetics [1,2]. These steels are preferred for demanding environments and critical applications due to their ease of cleaning and maintenance and their ability to maintain their mechanical properties under extreme conditions [3,4].

Stainless steel is a ferrous alloy characterized by low-carbon steel. It contains 10.5% chromium by weight, making it a corrosion-resistant alloy. In its chemical composition, stainless steel may contain other alloying elements such as nickel (Ni), molybdenum (Mo), nitrogen (N), or titanium (Ti), among others. The addition of these alloying elements improves the performance of these steels. Their appearance, formability, and mechanical or thermal resistance allow improvements to their behavior under high temperatures. Stainless steels are classified into five different families or types known as austenitic, ferritic, martensitic, duplex, and precipitation-hardening, and the latter is based on the type of heat treatment used and on the crystalline structure [4–7].

Precipitation-hardening stainless steels (PHSSs) are characterized by the mechanical resistance obtained from hardening by aging heat treatment. They are iron–chromium–nickel alloys. In the aeronautical sector, the most commonly used PHSSs are 15-5PH, 17-7PH, 17-4PH, Custom 450, and AM350, and they are manufactured for components such as blades, rotors, and turbine shafts, as well as structural components of aircraft [8–11].

Stainless steels stand out for their corrosion resistance, unlike conventional steel, which oxidizes and forms a reddish rust layer under normal conditions. This is because chromium adheres to oxygen to form a thin, transparent film of chromium oxide on the surface of the steel. This oxidation film is known as the passive layer, which prevents the further oxidation of the stainless steel. In the case of mechanical or chemical damage, the passive layer can be repaired autonomously in the presence of oxygen [12–16].

A literature review shows that nitric acid (HNO_3) is a powerful oxidant that facilitates the creation of passive films on stainless steels during the passivation process [11]. Nitric acid must be highly concentrated to be effective. However, many questions have been raised regarding the production of harmful-to-health toxic vapors by nitric acid in passivation baths. Moreover, the traditional disposal of used nitric acid presents environmental problems due to the generation of nitrates in wastewater and toxic sludge containing heavy metals. However, in recent years, alternative solutions have emerged that are non-toxic and environmentally sustainable, such as citric acid ($\text{C}_6\text{H}_8\text{O}_7$), which is inexpensive and can be extracted from fruits and vegetables. $\text{C}_6\text{H}_8\text{O}_7$ is frequently used in solutions around 20%, while HNO_3 can reach solutions of 40% based on international regulations. Since 2008, NASA and Boeing have reported research into passivating stainless steels in the presence of citric acid to improve corrosion resistance [17–22].

Direct and alternating current electrochemical techniques have been used to characterize the electrochemical behavior of various passivated stainless steels. Electrochemical impedance spectroscopy (EIS) is a technique that allows us to understand the corrosion mechanism, analyze the oxide layer, and establish the system's kinetics [23].

In 2004, the corrosion behavior of stainless steels with various molybdenum contents in solutions with and without oxygen was studied, where it was concluded that the presence of certain alloying elements, such as molybdenum, caused a decrease in the pH of the solutions [24]. The same authors, in 2007, investigated the growth of the chromium oxide film in passivated SS where the alloying elements determined the stability of the oxidation film [25]. Bragaglia et al. presented results on aeronautical components of stainless steels passivated with citric acid, indicating that the corrosion kinetics decreased compared to nitric acid [26]. According to the research of Marcelin et al. [27], the properties of the passive film control the electrochemical process of corrosion in martensitic stainless steels. Lara et al., in 2020, used electrochemical techniques such as potentiodynamic polarization curves and electrochemical noise to compare austenitic stainless steel 304 against 15-5PH and 17-4PH in citric and nitric acid baths and immersed in NaCl and H_2SO_4 . The corrosion kinetics were lower when citric acid was used [28]. In recent studies, Gaona et al. [1,6,8,9,23] have investigated the localized corrosion of PHSSs in acid baths using electrochemical

techniques, such as cyclic potentiodynamic polarization, electrochemical noise analysis in time, frequency, and time–frequency, and electrochemical impedance spectroscopy.

The present work aims to investigate the effect of citric acid at different concentrations (citric acid, citric acid + oxalic acid; citric acid + hydrogen peroxide and citric acid + hydrogen peroxide + ethanol) on AM 350 stainless steel passivated for 90 and 120 min at 25 and 50 °C and immersed in 5 wt. % sodium chloride solution, using electrochemical impedance spectroscopy (EIS) based on ASTM-G106. Stainless steels such as AM350 are used in the aeronautical industry and are exposed to different atmospheres such as marine and industrial environments.

2. Materials and Methods

2.1. Materials

The stainless steel used was AM 350 (AMS 5548; Aerospace Material Specifications) in the shape of 2-inch cylindrical bars. The nominal chemical composition is reported in Table 1. AM 350 is a chromium–nickel–molybdenum stainless steel that can be hardened by martensitic transformation or precipitation hardening. AM 350 may have an austenitic phase for best formability or a martensitic microstructure with high strength depending on the heat treatment. In the annealed condition, alloy AM 350 is essentially austenitic, forming characteristics similar to those of the AISI 300 series stainless steels. It has a higher rate of work hardening, and cold forming will cause martensite formation proportionate to the amount of deformation [23].

Table 1. The chemical composition of the AM 350 (wt.%) [29].

Element	AM 350
Fe	Balance
C	0.07–0.11
Cr	16.0–17.0
Ni	4.0–5.0
Mo	2.50–3.25
Mn	0.50–1.25
N	0.07–0.13
Si	≤0.50
S	0.030

The samples were cut from a cylindrical bar with a diameter of 2 inches [30]. Subsequently, all samples were prepared by metallography technique (for grinding and polishing, we employed 400-, 500-, 600-, and 800-grade SiC sandpaper) as indicated in the ASTM E3 [31]; the cleaning of the samples was performed by ultrasound [32] using an ethyl alcohol solution and a rinse with distilled water and air, respectively.

2.2. Passivation Treatment

In the passivation treatment, we controlled parameters such as bath concentration, temperature, and immersion times based on the SAE/ASM2700 and ASTM G967 standards [33–35]; see Figure 1.

- i. Passivated AM 350 steel samples were cleaned by ultrasound (10 min in ethanol) and immersed in deionized water.
- ii. The passivation baths used were as follows:
 - a. citric acid ($C_6H_8O_7$) 25% p/v;
 - b. citric acid ($C_6H_8O_7$) 25% p/v + oxalic acid ($C_2H_2O_4$) 10% v/v;

- c. citric acid ($C_6H_8O_7$) 25% p/v + hydrogen peroxide (H_2O_2) 10% v/v;
 - d. citric acid ($C_6H_8O_7$) 25% p/v + hydrogen peroxide (H_2O_2) 10% v/v + ethane (C_2H_6O) 5% v/v.
- iii. The bath temperatures were 25 and 50 °C, and the immersion times were set at 90 and 120 min.
 - iv. The samples were rinsed with deionized water and air-dried to finish the treatment.

The nomenclature used to identify each of the passivated samples is given in the following Table 2.

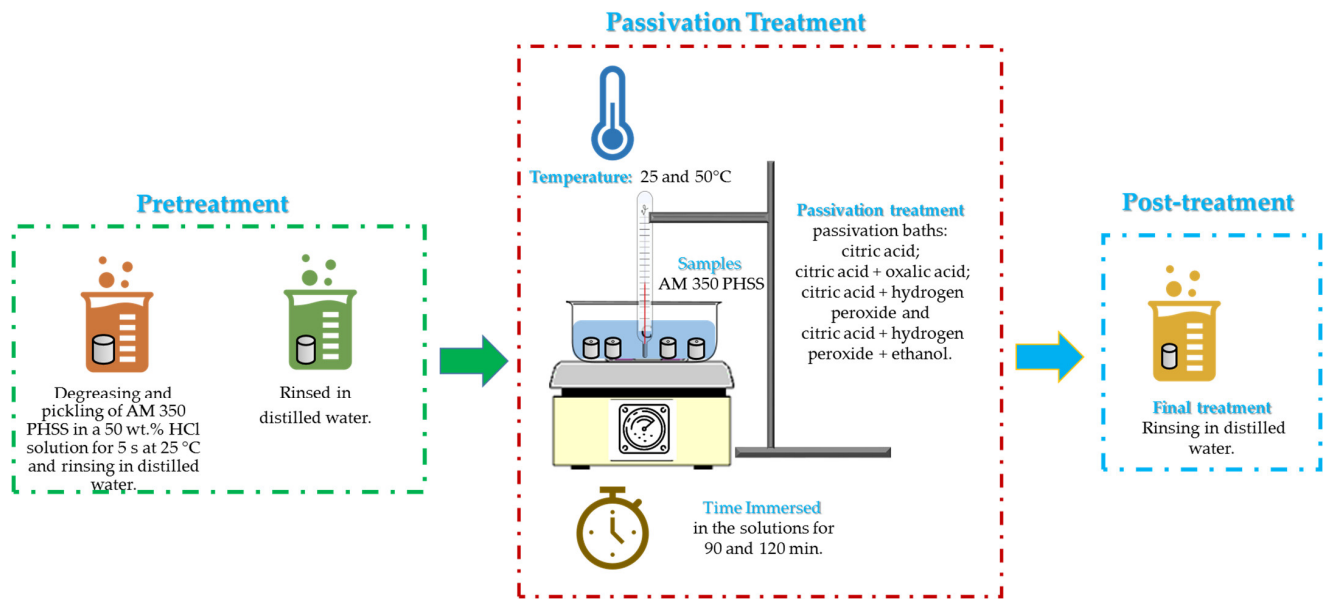


Figure 1. Diagram of passivation treatment of AM 350 PHSS.

Table 2. Nomenclature of the AM 350 samples.

Passivation Baths	Temperature (°C)	Concentration	Time (min)
citric acid ($C_6H_8O_7$)	25 and 50	($C_6H_8O_7$) 25% p/v	90 and 120
citric acid ($C_6H_8O_7$) + oxalic acid ($C_2H_2O_4$)	25 and 50	($C_6H_8O_7$) 25% p/v + ($C_2H_2O_4$) 10% v/v	90 and 120
citric acid ($C_6H_8O_7$) + hydrogen peroxide (H_2O_2)	25 and 50	($C_6H_8O_7$) 25% p/v + (H_2O_2) 10% v/v	90 and 120
citric acid ($C_6H_8O_7$) + hydrogen peroxide (H_2O_2) + ethane (C_2H_6O)	25 and 50	($C_6H_8O_7$) 25% p/v + (H_2O_2) 10% v/v + (C_2H_6O) 5% v/v	90 and 120

2.3. Corrosion Measurements

A three-electrode electrochemical cell (Figure 2) configuration was used for the corrosion measurements, with the working electrode (material to analyze), a saturated calomel electrode (SCE) as a reference electrode, and a platinum wire as a counter electrode. The tests were carried out in duplicate at room temperature using a Potentiostat/Galvanostat/ZRA (produced by Solartron 1287A, Bognor Regis, UK). The tests were evaluated in solutions containing 5 wt. % NaCl solution. The parameters used in the electrochemical impedance spectroscopy (EIS) technique included a frequency range of 0.01 to 100,000 Hz, the application of a 10 mV RMS amplitude, and 35 points per decade [36]. The results analysis was performed utilizing “Zview-4” software (<https://www.scribner.com/software/68-general-electrochemistr376-zview-for-windows/> Scrib-

nerAssociates, Inc. by Berek Johnson, Southern Pines, NC, USA), and the EIS diagrams were examined in terms of electrical equivalent circuits.

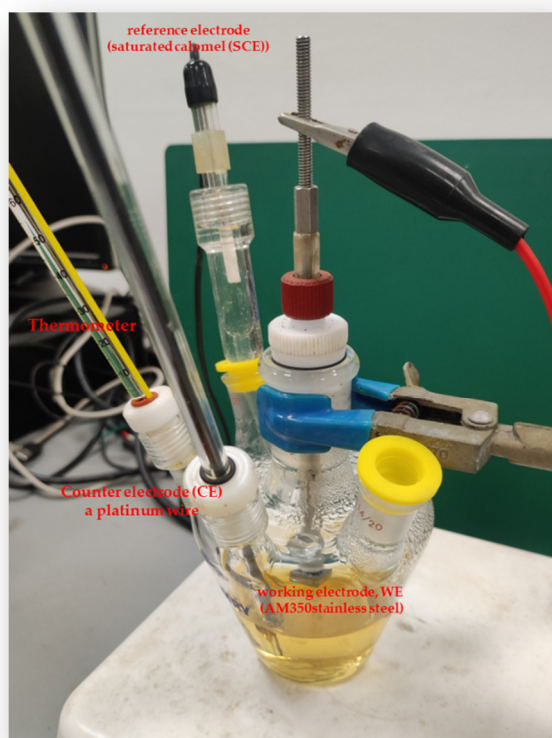


Figure 2. Conventional three-electrode corrosion cell.

2.4. Microstructural Characterization

Scanning electron microscopy (SEM, JEOL-JSM-5610LV, Tokyo, Japan) was used to determine the microstructure of AM 350 PHSS, using the secondary electron (SE) detector at 500 \times , operating at 20 kV, WD = 14 mm.

3. Results

3.1. SEM Microstructural Analysis

The SEM technique was used to study the microstructures of the AM 350 PHSS in initial conditions. Figure 3 shows an SEM-SE micrograph of AM 350 SS (a) containing austenite (γ) and delta (δ) ferrite phase, respectively, and an EDS Spectrum (b) in which the presence of alloying elements such as chromium, nickel, iron, silicon and carbon can be observed. The presence of austenite (γ) in semi-austenitic steels is a thermodynamically stable phase that can be transformed by an aging treatment. Likewise, alloying elements were found to indicate the presence of the delta ferrite (δ) phase [16,23].

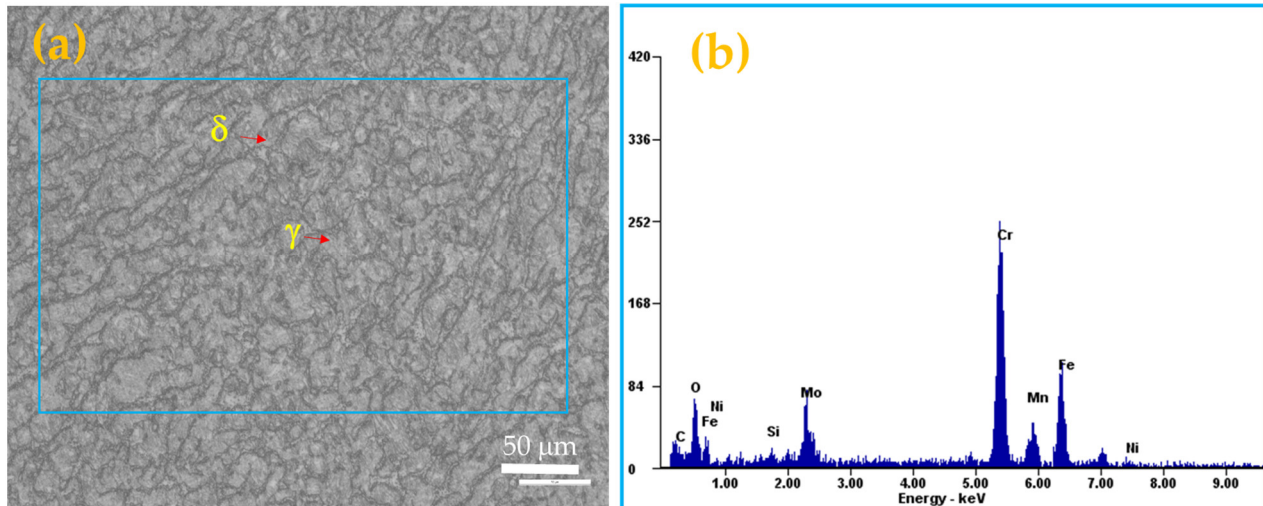


Figure 3. SEM-SE (a) microstructures of AM 350SS, initial condition, and (b) EDS spectrum.

3.2. Electrochemical Impedance Spectroscopy (EIS)

Our investigation into AM350 stainless steel passivated in different concentrations of citric acid allowed us to observe the effect on localized corrosion. The interpretation of EIS data, based on Nyquist and Bode diagrams, is the subject of various theories and models for simulating experimental data. Their physical interpretation was enhanced by using equivalent circuits, which are models that seek to interpret and relate each element of the electrical circuit with the electrochemical phenomena that occur at the metal/film and film/solution interfaces, as well as within the film. These models provide kinetic information on corrosion and a mechanistic study on the growth and degradation of the passive film [37–39].

According to the structure of the oxide layer, two equivalent circuits were proposed that model the system's behavior, which can be seen in Figure 4. The equivalent circuit models are the ones that best fit the Nyquist diagrams of the passivated stainless steel samples exposed to a 5 wt. % NaCl solution, where R_s represents the electrolyte resistance, CPE_1 and CPE_2 represent the constant phase element of the porous layer and the protective layer for the passivated film, and R_1 corresponds to the resistance of the porous layer and R_2 to the resistance of the protective layer. The CPEs, constant phase elements, represent the impedance response for electrochemical systems in corrosion and often reflect a reactivity distribution [40–43]. The simple Faradaic reaction without diffusion can be defined in terms of a CPE, as indicated in the following Equation (1):

$$Z(\omega) = R_s + \frac{R_{ct}}{1 + (j\omega)^\alpha Q R_{ct}} \quad (1)$$

The ohmic resistance is R_s , and the charge transfer resistance is identified as R_{ct} . The parameters α and Q (CPE) are frequency-independent. When $\alpha = 1$, Q has capacitance units ($\mu\text{F}\cdot\text{cm}^{-2}$), representing the interface capacitance. When $\alpha < 1$, the electrochemical system exhibits behavior attributed to its heterogeneity or continuously distributed time constants for charge transfer reactions. Regardless of the cause of the CPE behavior, the phase angle associated with CPE is frequency-independent and is expressed in Equation (2) [44].

$$Z(\omega) = R_e + \frac{1}{(j\omega)^\alpha Q} \quad (2)$$

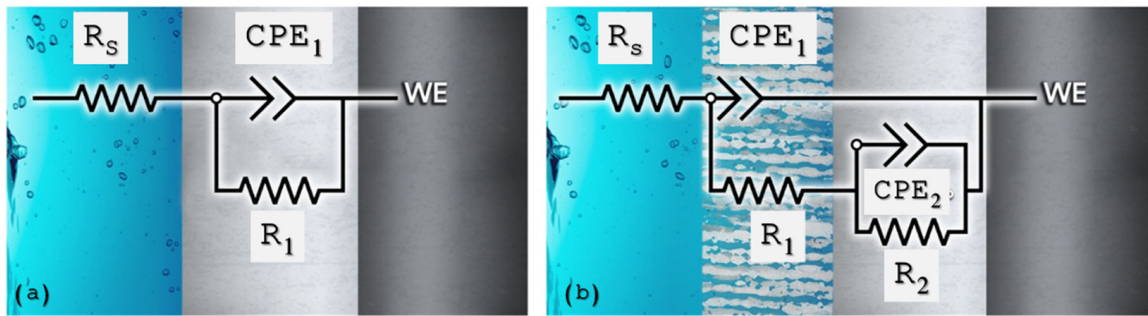


Figure 4. The proposed electrical equivalent circuit (EEC) model. Systems of (a) one time constant and (b) two time constants.

Figure 5 shows the Nyquist and Bode diagrams of AM350 passivated in citric acid exposed to NaCl electrolyte. The figure shows how C/25/25/120 presented a higher resistance to corrosion in Nyquist and Bode $|Z|$ diagrams, obtaining values of $3 \times 10^5 \Omega \cdot \text{cm}^2$, and the sample C/50/25/120 presented the lower corrosion resistance, with values of $1.5 \times 10^5 \Omega \cdot \text{cm}^2$. The equivalent circuit in Figure 3 shows how two time constants are present for all samples except the sample C/50/25/90, which only presents one time constant. The first layer is related to the passive layer, where the highest resistance is for C/25/25/120; that resistance is associated with R_{ct} ($14,283 \Omega \cdot \text{cm}^2$) (see Table 3). The CPE in the first layer is $8.49 \times 10^{-6} \mu\text{F}/\text{cm}^2$. The values obtained for n are of the order of 0.8, indicating that the behavior is associated with the capacitive system of a double layer. Also, this value indicates that the passive layer created is homogenous. The behavior of n in the second time constant is near 0.5, which indicates that impeded diffusion is occurring, so the generation of oxide by a diffusion model is not occurring due to non-homogenous ion transfer. All the samples presented CPE_1 values of the $\times 10^{-5} \text{ F}/\text{cm}^2$ order; however, the lowest value was C/25/25/120, indicating that the passive layer has acceptable conditions against corrosion.

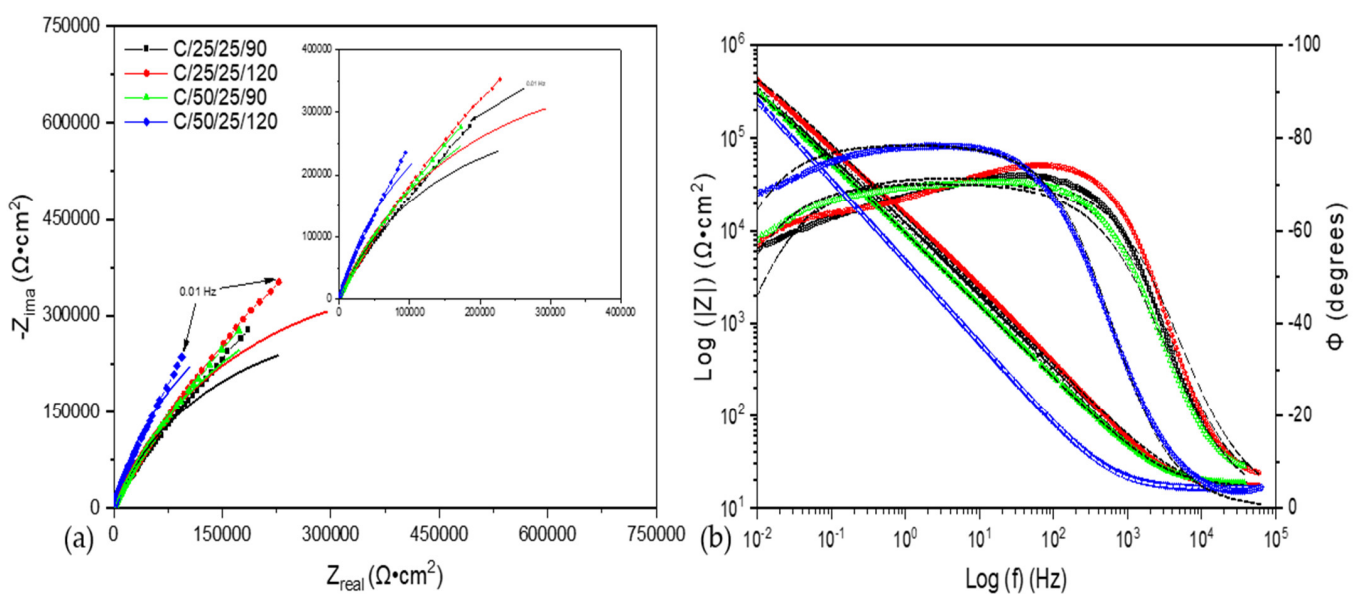


Figure 5. Nyquist (a) and Bode (b) diagrams were obtained for AM 350 samples in a citric acid bath ($\text{C}_6\text{H}_8\text{O}_7$) and immersed in 5 wt. % NaCl solution.

Table 3. Electrochemical characteristics from Nyquist diagrams of AM 350 samples in a citric acid ($C_6H_8O_7$) bath and immersed in 5 wt. % NaCl solution.

Sample	R_{sol} ($\Omega \cdot cm$)	CPE_1 ($\mu F/cm^2$)	n_1	R_1 ($\Omega \cdot cm$)	CPE_2 ($\mu F/cm^2$)	n_2	R_2 ($\Omega \cdot cm$)	χ^2
C/25/25/90	17 ± 1.5	$1.45 \times 10^{-5} \pm 1.5 \times 10^{-7}$	0.84 ± 0.1	$11,360 \pm 40$	$8.16 \times 10^{-6} \pm 2 \times 10^{-8}$	0.59 ± 0.05	$1,994,500 \pm 58$	5.4×10^{-4}
C/25/25/120	16 ± 2.0	$1.01 \times 10^{-5} \pm 2.1 \times 10^{-7}$	0.86 ± 0.1	$14,283 \pm 11$	$8.49 \times 10^{-6} \pm 1 \times 10^{-8}$	0.62 ± 0.05	$3,654,800 \pm 63$	5.0×10^{-4}
C/50/25/90	17 ± 1.3	$2.06 \times 10^{-5} \pm 1.6 \times 10^{-7}$	0.81 ± 0.1	$13,204 \pm 20$	$5.62 \times 10^{-6} \pm 1.8 \times 10^{-8}$	0.65 ± 0.05	$1,383,400 \pm 87$	6.4×10^{-4}
C/50/25/120	16 ± 0.9	$4.29 \times 10^{-5} \pm 2.2 \times 10^{-7}$	0.88 ± 0.1	$962,470 \pm 23$	-	-	-	1.9×10^{-3}

Figure 6 shows the Nyquist and Bode diagrams for AM350 passivated in citric and oxalic acid exposed to a NaCl solution. The results show (see Table 4) how C.O/25/25.10/120 presents values of $7 \times 10^5 \Omega \cdot cm^2$ according to the Bode $|Z|$ diagram. On the other hand, C.O/50/25.10/120 presents a resistance of $2 \times 10^5 \Omega \cdot cm^2$. That behavior can be observed in the Nyquist diagram, with a high semicircle value for C.O/25/25.10/120. The samples C.O/25/25.10/90 and C.O/25/25.10/120 present a double-layer behavior; both samples present similar resistance with values of $2.7 \times 10^4 \Omega \cdot cm^2$, the capacitive values are also of the order of $\times 10^{-5} \mu F/cm^2$. The value of the first n is 0.86 and 0.87, indicating that a homogenous passive layer is formed; on the other hand, the second value of R is $20 \times 10^5 \Omega \cdot cm^2$ for C.O/25/25.10/90 and $50 \times 10^5 \Omega \cdot cm^2$ for C.O/25/25.10/120, with an n value of 0.76 and 0.65. These values are associated with the possibility of a secondary passive layer at the interface of metal; for sample C.O/25/25.10/120, the value of 0.65 indicates that the surface is heterogeneous and that an impeded diffusion occurs. For sample C.O/25/25.10/90, the value of 0.75 indicates that the surface is heterogeneous. Therefore, the resistance of C.O/25/25.10/120 is higher than that of C.O/25/25.10/90. The CPE values are of the $\times 10^{-5} F/cm^2$ order in the first layer, and in the second, they decrease to $\times 10^{-6}$; the lower value indicates that the resistance to ionic transference is higher.

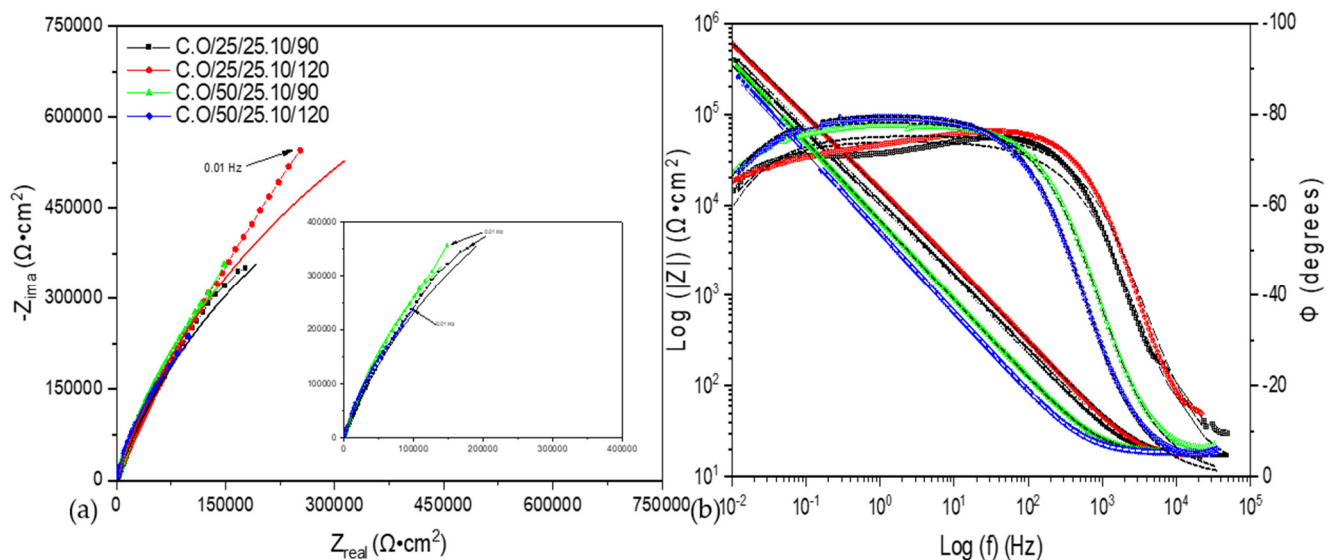
**Figure 6.** Nyquist (a) and Bode (b) diagrams obtained for AM 350 samples in citric acid ($C_6H_8O_7$) + oxalic acid ($C_2H_2O_4$) bath immersed in 5 wt. % NaCl solution.

Figure 7 shows the Nyquist and Bode diagrams of AM350 passivate in citric acid with hydrogen peroxide immersed in NaCl solution. Sample C.P/50/25.10/90 presents the highest resistance to corrosion: $4 \times 10^5 \Omega \cdot cm^2$. On the other hand, C.P/50/25.10/120 presents the lower corrosion resistance with values of $0.9 \times 10^5 \Omega \cdot cm^2$; however, it is the only sample that presents a double-layer behavior, with $14.52 \times 10^4 \Omega \cdot cm^2$, and an n of 0.94. This means that the passive layer created is more homogenous than the passive layer

of the sample mentioned in Figures 3 and 4. The other samples present the behavior of one time constant, indicating that the passive layer created only presents one interface (see Table 5). The CPE values are of the $\times 10^{-5}$ F/cm² order, but C.P/50/25.10/120 presents the highest value, with 4.07×10^{-5} F/cm², indicating that ionic transference is higher, so the corrosion resistance decreases.

Table 4. Electrochemical characteristics from Nyquist diagrams of AM 350 samples in citric acid (C₆H₈O₇) + oxalic acid (C₂H₂O₄) bath immersed in 5 wt. % NaCl solution.

Sample	R _{sol} (Ω·cm)	CPE ₁ (μF/cm ²)	n ₁	R ₁ (Ω·cm)	CPE ₂ (μF/cm ²)	n ₂	R ₂ (Ω·cm)	χ ²
C.O/25/25.10/90	15 ± 1	$1.65 \times 10^{-5} \pm 0.9 \times 10^{-7}$	0.86 ± 0.02	27,519 ± 21	$5.96 \times 10^{-6} \pm 1 \times 10^{-8}$	0.76 ± 0.02	2,063,800 ± 120	1.6×10^{-3}
C.O/25/25.10/120	15.81 ± 0.5	$1.16 \times 10^{-5} \pm 0.7 \times 10^{-7}$	0.87 ± 0.06	27,929 ± 36	$3.97 \times 10^{-6} \pm 0.6 \times 10^{-8}$	0.65 ± 0.02	5,091,900 ± 98	5.2×10^{-4}
C.O/50/25.10/90	17.91 ± 0.8	$3.00 \times 10^{-5} \pm 1.8 \times 10^{-7}$	0.87 ± 0.02	1,624,200 ± 240	-	-	-	1.1×10^{-3}
C.O/50/25.10/120	18.2 ± 0.4	$3.86 \times 10^{-5} \pm 1.3 \times 10^{-7}$	0.89 ± 0.03	1,022,800 ± 603	-	-	-	1.3×10^{-3}

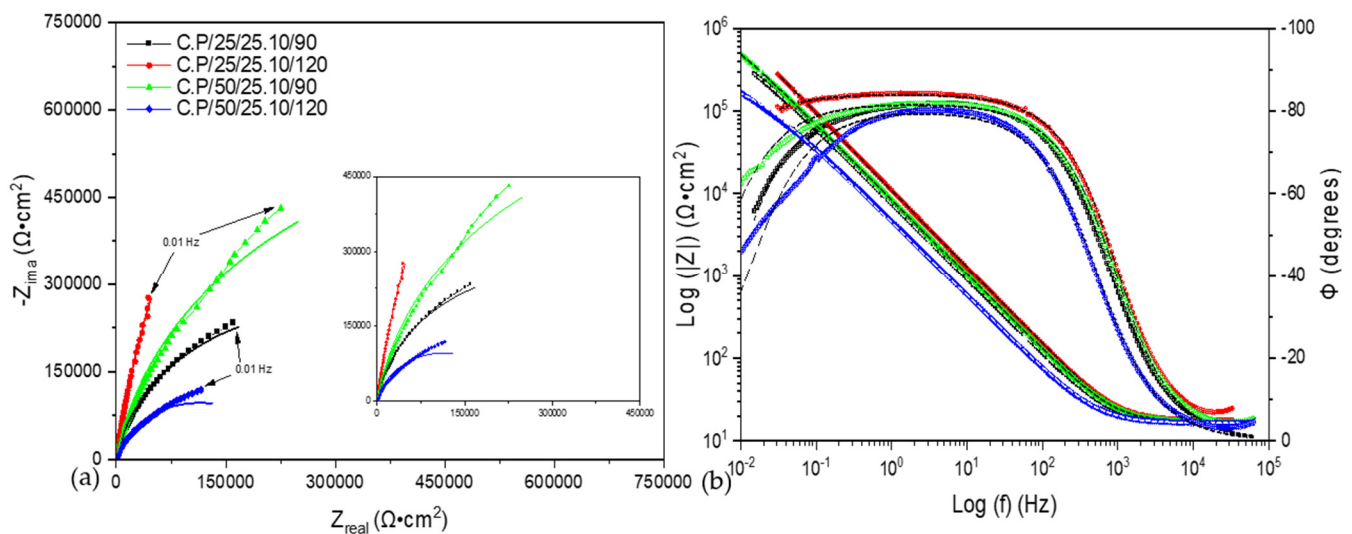


Figure 7. Nyquist (a) and Bode (b) diagrams obtained for AM 350 samples in citric acid (C₆H₈O₇) + hydrogen peroxide (H₂O₂) bath and immersed in 5 wt. % NaCl solution.

Table 5. Electrochemical characteristics from Nyquist diagrams of AM 350 samples in citric acid (C₆H₈O₇) + hydrogen peroxide (H₂O₂) bath and immersed in 5 wt. % NaCl solution.

Sample	R _{sol} (Ω·cm)	CPE ₁ (μF/cm ²)	n ₁	R ₁ (Ω·cm)	CPE ₂ (μF/cm ²)	n ₂	R ₂ (Ω·cm)	χ ²
C.P/25/25.10/90	16 ± 0.5	$2.50 \times 10^{-5} \pm 1 \times 10^{-7}$	0.91 ± 0.02	584,230 ± 86	-	-	-	1.0×10^{-3}
C.P/25/25.10/120	17 ± 0.8	$1.65 \times 10^{-5} \pm 2 \times 10^{-7}$	0.93 ± 0.02	4,155,700 ± 70	-	-	-	1.7×10^{-3}
C.P/50/25.10/90	16 ± 0.8	$2.24 \times 10^{-5} \pm 1 \times 10^{-7}$	0.91 ± 0.02	1,201,800 ± 63	-	-	-	1.2×10^{-3}
C.P/50/25.10/120	16 ± 0.9	$4.07 \times 10^{-5} \pm 1 \times 10^{-7}$	0.94 ± 0.02	145,210 ± 23	$7.67 \times 10^{-5} \pm 1.6 \times 10^{-7}$	0.92 ± 0.02	130,830 ± 17	5.5×10^{-3}

Figure 8 shows the Nyquist and Bode diagrams of AM350 passivated in citric acid with hydrogen peroxide and ethane exposed to NaCl solution. In these samples, CPE/25/25.10.5/90 presents a higher impedance with values of 15.9×10^5 Ωcm²; in contrast, CPE/25/25.10/120 presents a lower resistance of 41.95×10^4 Ω·cm². The behavior of these samples is related to a one-time-constant system, and the values of n (Table 6) indicate that the passive layer is homogenous due to the value of 0.9, very near to 1, which would indicate perfect capacitance; for this reason, charge is distributed on the surface in a more homogenous way. Sample CPE/25/25.10.5/120 presents the higher CPE, with 3.99×10^{-5} F/cm², indicating that the ionic transference is higher than the other samples. This result is related to the lower corrosion resistance of the sample.

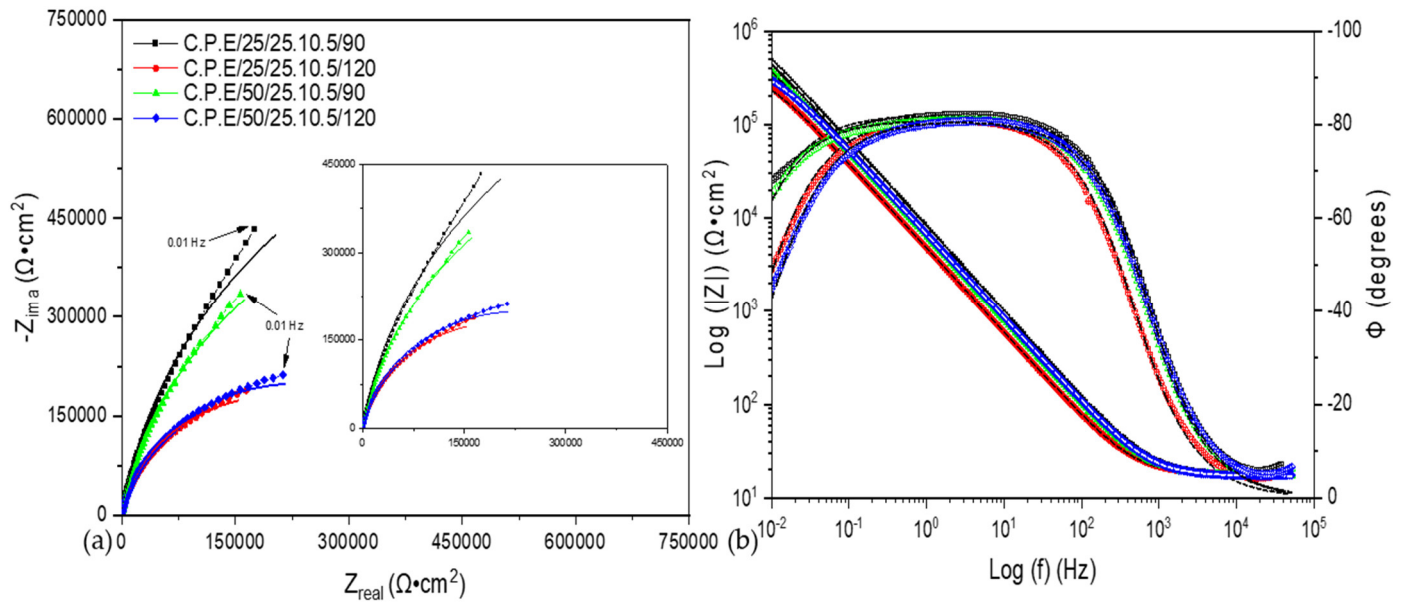


Figure 8. Nyquist (a) and Bode (b) diagrams obtained for AM 350 samples in citric acid ($C_6H_8O_7$) + hydrogen peroxide (H_2O_2) + ethane (C_2H_6O) bath and immersed in 5 wt. % NaCl solution.

Table 6. Electrochemical characteristics from Nyquist diagrams of AM 350 samples in citric acid ($C_6H_8O_7$) + hydrogen peroxide (H_2O_2) + ethane (C_2H_6O) bath and immersed in 5 wt. % NaCl solution.

Sample	R_{sol} ($\Omega\cdot cm$)	CPE_1 ($\mu F/cm^2$)	n_1	R_1 ($\Omega\cdot cm$)	χ^2
C.P.E/25/25.10.5/90	17 ± 0.5	$2.42 \times 10^{-5} \pm 6 \times 10^{-7}$	0.91 ± 0.15	$1,530,900 \pm 130$	1.7×10^{-3}
C.P.E/25/25.10.5/120	18 ± 0.3	$3.99 \times 10^{-5} \pm 7 \times 10^{-7}$	0.90 ± 0.17	$419,510 \pm 99$	1.6×10^{-3}
C.P.E/50/25.10.5/90	17 ± 0.5	$3.02 \times 10^{-5} \pm 3 \times 10^{-7}$	0.90 ± 0.15	$1,197,500 \pm 178$	1.1×10^{-3}
C.P.E/50/25.10.5/120	17 ± 0.2	$2.83 \times 10^{-5} \pm 4 \times 10^{-7}$	0.90 ± 0.1	$464,940 \pm 169$	1.1×10^{-3}

4. Discussion

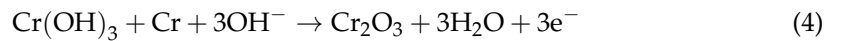
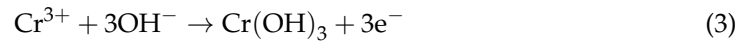
The AM350 steel presented a passive behavior and two corrosion systems. The first system showed a one-time-constant behavior, while the other presented a double-layer behavior, which is the most common in a system with a protective layer. The double-layer behavior occurs at low and medium frequencies due to a redox reaction on the material surface [43–46]. For some authors [47–49], a passive layer with only one time constant is associated with an unstable system due to the decomposition of the oxide layer. In a double-barrier system, after the dissolution of the first interface, a process of retained diffusion occurs for some samples, which indicates that an oxide layer is continuously being created; meanwhile, one time system indicates that the passive layer is degraded and the oxide generated by the corrosion process is unstable.

The one-time-constant system is associated with a metal dissolution up to the passivation process [50]; however, when one time constant presents n values of 0.9, this indicates that the surface is heterogenous and is not susceptible to pitting corrosion. For this reason, samples that present a layer system are more susceptible to localized corrosion [51], because the first layer is related to the passive layer and the second is related to the charge transfer and capacitance inside pits and cracks in the surface. Therefore, the n values of the second barrier are between 0.5 and 0.6, indicating a heterogenous surface and a retained diffusion process.

Double-layer systems are more connected to active pits because the surface area is inside. This behavior increases in the presence of Cl^- , which attacks preference zones; however, the formation of Cr oxides protects the material against corrosion. When samples

are submerged in NaCl solution, an unstable passivation film causes an increase in current density, affecting the corrosion kinetics of stainless steel [52–56].

It is important to consider that NaCl is not a passivation electrolyte; however, the behavior shown for samples with values for n near to 0.5 indicates that a diffusion process is retained, meaning that the material can be a pseudopassivate [57–61]. This occurs due to the generation of an oxide layer of Cr, as the following equation shows:



One time constant indicates that the material has a passive layer in constant active behavior. However, the values of n that are near 0.9 indicate that the passive layer generated is heterogeneous.

Figure 9 shows the results for the R_{ct} of each sample; this value is associated with the transference resistance and directly with the resistance of the passive layer. The sample anodized in citric acid + hydrogen peroxide shows higher corrosion resistance. This behavior is associated with revisiting hydrogen peroxide, which generates a redox process; however, the oxide layer created is more stable. The corrosion resistance increases when time increases for this passivation bath, which means that the passive layer is more stable when the time is longer and the temperature is 25 °C.

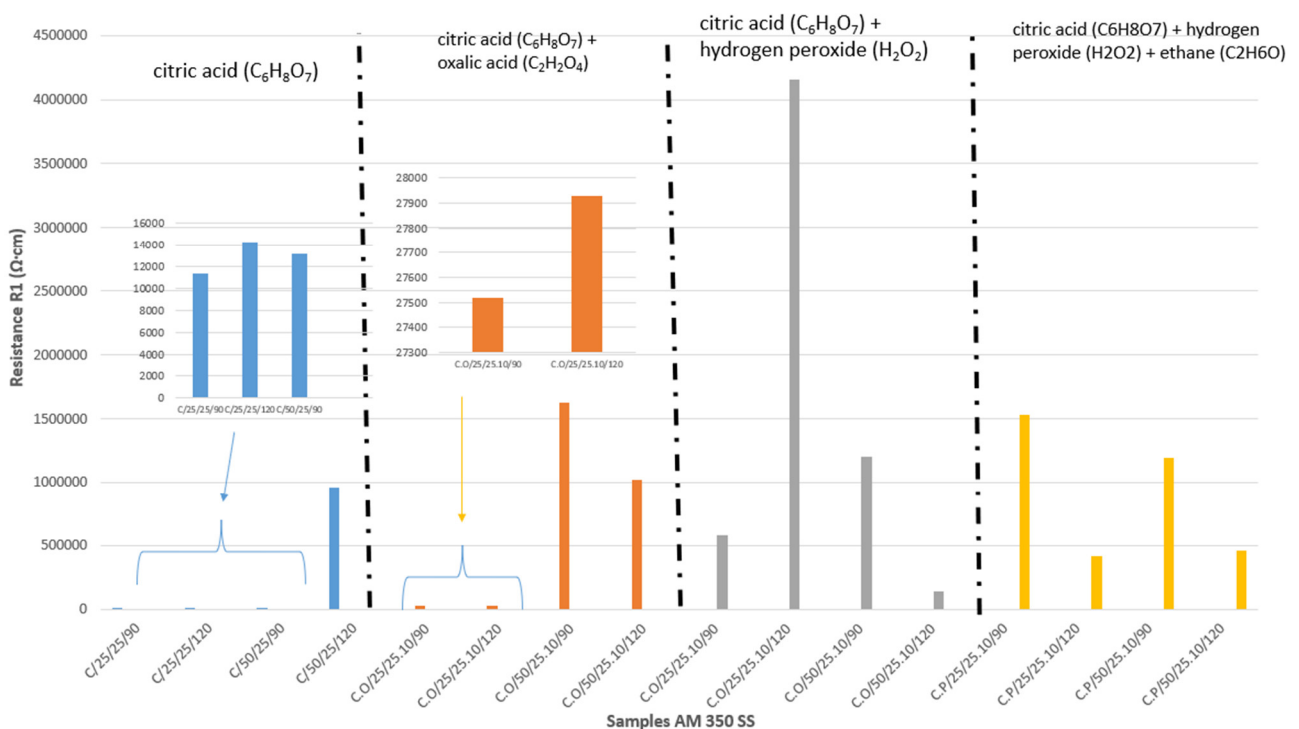


Figure 9. Diagram comparing the R_1 or R_{ct} value of each sample passivated in the different media.

The effect of temperature can be observed for samples passivated in citric + oxalic acid, where the temperature increases R_{ct} resistance. This behavior is related to the catalytic effect of temperature. However, that effect is contradictory for citric acid + hydrogen peroxide and citric acid + hydrogen peroxide + ethane, where temperature leads to a decrease in the corrosion resistance of the passive layer. This occurs when the high temperature generates an increase in passive layer vacancies [62–64].

For this reason, it is difficult to determine a temperature and time homogenous for all baths because each one leads to different properties in the passive layer.

5. Conclusions

After studying the corrosion behavior of AM350 stainless steels passivated in citric acid at different concentrations (citric acid; citric acid + oxalic acid; citric acid + hydrogen peroxide and citric acid + hydrogen peroxide + ethanol) for 90 and 120 min at 25 and 50 °C and exposed to 5 wt. % sodium chloride solution and using electrochemical impedance spectroscopy, the following conclusions can be drawn:

- The impedance parameters provided relevant information concerning the role of chlorides and corrosion resistance.
- The equivalent circuit presented a one-time-constant and two-time-constant corrosion system.
- The results indicate that a two-time-system or double-layer equivalent circuit is associated with a system that is susceptible to pitting due to the behavior of the second barrier, where the n values are 0.6, indicating that the second layer is heterogeneous due to cracks and pittings.
- The AM 350 stainless steels passivated in citric and oxalic acid presented the higher corrosion resistance with values of $6 \times 10^5 \Omega \cdot \text{cm}^2$ for sample C.O/25/25.10/120, indicating that with an increase in time, the passivate will be generated in a better way.
- After evaluation using EIS, it was observed that adding peroxide and ethanol helped to make the passivation process more stable at 50 °C because when passivation was performed in that media, the corrosion resistance increased when the passivation temperature increased. However, when the time increased, the corrosion resistance decreased.
- The citric acid passivation process in stainless steels could represent an environmentally friendly alternative to the frequently used nitric acid passivation process.

Author Contributions: Conceptualization, C.G.-T.; F.A.-C., and M.V.-T.; methodology, M.V.-T., M.A.B.-Z., C.T.M.-R., A.L.-G., M.L.-B., J.M.J.-M., and E.M.-B.; data curation, F.A.-C., D.N.-M., C.T.M.-R., A.L.-G., C.G.-T.; V.A.-C., and formal analysis, C.G.-T.; F.A.-C., M.L.-B., E.M.-B., M.A.B.-Z., D.N.-M., V.A.-C., and E.M.-B.; writing—review and editing, C.G.-T.; J.M.J.-M., and F.A.-C. All authors have read and agreed to the published version of the manuscript.

Funding: This research received no external funding.

Institutional Review Board Statement: Not applicable.

Informed Consent Statement: Not applicable.

Data Availability Statement: The original contributions presented in this study are included in the article. Further inquiries can be directed to the corresponding authors.

Acknowledgments: The authors wish to thank the Academic Body UANL—CA-316 “Deterioration and integrity of composite materials” and Universidad Autónoma de Nuevo León (UANL) for the facilities provided for this investigation.

Conflicts of Interest: The authors declare no conflicts of interest.

References

1. Villegas-Tovar, J.; Gaona-Tiburcio, C.; Lara-Banda, M.; Maldonado-Bandala, E.; Baltazar-Zamora, M.A.; Cabral-Miramontes, J.; Nieves-Mendoza, D.; Olguin-Coca, J.; Estupiñan-Lopez, F.; Almeraya-Calderón, F. Electrochemical Corrosion Behavior of Passivated Precipitation Hardening Stainless Steels for Aerospace Applications. *Metals* **2023**, *13*, 835. [[CrossRef](#)]
2. Gialanella, S.; Malandrucolo, A. *Aerospace Alloys*; Topics in Mining, Metallurgy and Materials Engineering; Bergmann, C.P., Ed.; Springer: Cham, Switzerland, 2020; ISSN 2364-3307. [[CrossRef](#)]
3. Mouritz, P.A. *Introduction to Aerospace Materials*; Woodhead Publishing: Cambridge, UK, 2012.

4. Koch, G.H.; Brongers, M.P.H.; Thompson, N.G.; Virmani, P.Y.; Payer, J.H. Chapter 1: Costs of corrosion in the United States. In *Handbook of Environmental Degradation of Materials*; Kutz, M., Ed.; William Andrew: New York, NY, USA, 2005; pp. 3–24.
5. Chatterjee, M.; Patra, A.; Babu, R.; Narayana, R. *Aerospace Materials and Technologies Volume 2: Aerospace Materials and Material Technologies*, 1st ed.; Prasad Esvara, N., Wanhill, R.J.H., Eds.; Springer Science + Business Media: Singapore, 2017; pp. 3–24.
6. Banda, M.L.; Gaona-Tiburcio, C.; Zambrano-Robledo, P.; Cabral, M.J.A.; Estupinan, F.; Baltazar-Zamora, M.A.; Almeraya-Calderon, F. Corrosion Behaviour of 304 Austenitic, 15-5PH and 17-4PH Passive Stainless Steels in acid solutions. *Int. J. Electrochem. Sci.* **2018**, *13*, 10314–10324. [[CrossRef](#)]
7. Cobb, H.M. *The History of Stainless Steel*; ASM International: Novelt, OH, USA, 2010.
8. Samaniego-Gómez, O.; Almeraya-Calderón, F.; Chacón-Nava, J.; Maldonado-Bandala, E.; Nieves-Mendoza, D.; Flores-De los Rios, J.P.; Jáquez-Muñoz, J.M.; Delgado, A.D.; Gaona-Tiburcio, C. Corrosion Behavior of Passivated CUSTOM450 and AM350 Stainless Steels For Aeronautical Applications. *Metals* **2022**, *12*, 666. [[CrossRef](#)]
9. Almeraya-Calderon, F.; Villegas-Tovar, M.; Maldonado-Bandala, E.; Lara-Banda, M.; Baltazar-Zamora, M.A.; Santiago-Hurtado, G.; Nieves-Mendoza, D.; Lopez-Leon, L.D.; Jaquez-Muñoz, J.M.; Estupiñán-López, F.; et al. Use of Electrochemical Noise for the Study of Corrosion by Passivated CUSTOM 450 and AM 350 Stainless Steels. *Metals* **2024**, *14*, 341. [[CrossRef](#)]
10. Lopes, J.C. Material selection for aeronautical structural application. *Sci. Technol. Adv. Mat.* **2008**, *20*, 78–82.
11. Lo, K.H.; Shek, C.H.; Lai, J.K.L. Recent developments in stainless steels. *Mat. Sci. Eng. R.* **2009**, *65*, 39–104. [[CrossRef](#)]
12. Gaona-Tiburcio, C.; Montoya, R.M.; Cabral, M.J.; Estupiñán, L.F.; Zambrano, R.P.; Orozco, C.R.; Chacon-Nava, J.; Baltazar Z, M.; Almeraya-Calderon, F. Corrosion Resistance of Multilayer Coatings Deposited by PVD on Inconel 718 Using Electrochemical Impedance Spectroscopy Technique. *Coatings* **2020**, *10*, 521. [[CrossRef](#)]
13. Farrar, J. *The Alloy Tree—A Guide to Low-Alloy Steels, Stainless Steels and Nickel-Base Alloys*; Woodhead Publishing Limited and CRC Press: Sawston, UK, 2004.
14. ASM International. Introduction to Stainless Steel. In *Alloy Digest Sourcebook—Stainless Steel*, 3rd ed.; David, J.R., Davis & Associates, Eds.; ASM International: Novelt, OH, USA, 2000; pp. 2–3.
15. Almeraya-Calderón, F.; Samaniego-Gómez, O.; Maldonado-Bandala, E.; Nieves-Mendoza, D.; Olgún-Coca, J.; Jáquez-Muñoz, J.M.; Cabral-Miramontes, J.; Flores-De los Rios, J.P.; Bautista-Margulis, R.G.; Gaona-Tiburcio, C. Corrosion Behavior of Passivated Martensitic and Semi-Austenitic Precipitation Hardening Stainless Steel. *Metals* **2022**, *12*, 1033. [[CrossRef](#)]
16. Almeraya-Calderón, F.; Villegas-Tovar, M.; Maldonado-Bandala, E.; Lara-Banda, M.; Baltazar-Zamora, M.A.; Landa-Ruiz, L.; Nieves-Mendoza, D.; Jaquez-Muñoz, J.M.; Estupiñán-Lopez, F.; Cabral-Miramontes, J.; et al. Localized Corrosion of CUSTOM 450 and AM 350 Stainless Steels in H₂SO₄ and NaCl Solutions. *Materials* **2025**, *18*, 988. [[CrossRef](#)]
17. Gaydos, S.P. Passivation of aerospace stainless parts with citric acid solutions. *Plat. Surf. Finish.* **2003**, *90*, 20–25.
18. Schweitzer, P.A. *Metallic Materials: Physical, Mechanical, and Corrosion Properties*; M. Dekker: New York, NY, USA, 2003.
19. Benavides, S. *Corrosion Control in the Aerospace Industry*; Woodhead Publishing: Cambridge, UK, 2009.
20. Lewis, P.; Kolody, M. Alternative to Nitric Acid Passivation of Stainless Steel Alloys. In Technology Evaluation for Environmental Risk Mitigation Compendium, Proceedings of the NASA Technology Evaluation for Environmental Risk Mitigation Principal Center (TEERM), Kennedy Space Center, FL, USA, 13 January 2008; Department of Defense (DoD) and NASA, Kennedy Space Center: Merritt Island, FL, USA, 2008.
21. *ASTM A967-17*; Standard Specification for Chemical Passivation Treatments for Stainless Steel Parts. ASTM International: West Conshohocken, PA, USA, 1999.
22. NASA. Technical Reports Server. Available online: <https://ntrs.nasa.gov/citations/19680010964> (accessed on 15 May 2024).
23. Gaona Tiburcio, C.; Samaniego Gómez, O.; Jáquez Muñoz, J.M.; Baltazar Zamora, M.A.; Landa-Ruiz, L.; Lira Martínez, A.; Flores De los Rios, J.P.; Cabral Miramontes, J.; Estupinán-López, F.; Almeraya Calderon, F. Frequency-Time Domain Analysis of Electrochemical Noise of Passivated AM350 Stainless Steel for Aeronautical Applications. *Int. J. Electrochem. Sci.* **2022**, *17*, 220950. [[CrossRef](#)]
24. El-Taib Heakal, F.; Ameer, M.A.; El-Aziz, A.M.; Fekry, A.M. Electrochemical behavior of Mo-containing austenitic stainless steel in buffer solutions. *Mater. Werkst.* **2004**, *35*, 407–413. [[CrossRef](#)]
25. El-Taib Heakal, F.; Ghoneim, A.; Fekry, A. Stability of spontaneous passive films on high strength Mo-containing stainless steels in aqueous solutions. *J. Appl. Electrochem.* **2007**, *37*, 405–413. [[CrossRef](#)]
26. Bragaglia, M.; Cherubini, V.; Cacciotti, I.; Rinaldi, M.; Mori, S.; Soltani, P.; Nanni, F.; Kaciulis, S.; Montesperelli, G. Citric Acid Aerospace Stainless Steel Passivation: A Green Approach. In Proceedings of the CEAS Aerospace Europe Conference 2015, Delft, The Netherlands, 7–11 September 2015.
27. Marcelin, S.; Pébèrea, N.; Régnierb, S. Electrochemical characterisation of a martensitic stainless steel in a neutral chloride solution. *Electrochim. Acta* **2013**, *87*, 32–40. [[CrossRef](#)]
28. Lara-Banda, M.; Gaona-Tiburcio, C.; Zambrano-Robledo, P.; Delgado-E., M.; Cabral-Miramontes, J.; Nieves-Mendoza, D.; Maldonado-Bandala, E.; Estupiñán-Lopez, F.; Chacón-Nava, J.; Almeraya-Calderón, F. Alternative to Nitric Acid Passivation of 15-5 and 17-4PH Stainless Steel Using Electrochemical Techniques. *Materials* **2020**, *13*, 2836. [[CrossRef](#)]

29. AM 350 Technical Data. Available online: <https://www.hightempmetals.com/techdata/hitempAM350data.php> (accessed on 30 November 2024).
30. *ASTM A380-17*; Standard Practice for Cleaning, Descaling and Passivation of Stainless-Steel Parts, Equipment, and Systems. ASTM International: West Conshohocken, PA, USA, 1999.
31. *ASTM E3-95*; Standard Practice for Preparation of Metallographic Specimens. ASTM International: West Conshohocken, PA, USA, 1995.
32. Gallego-Juárez, J.A.; Graff, K.F. *Power Ultrasonics—Applications of High-Intensity Ultrasound*; Woodhead Publishing: Cambridge, UK, 2015.
33. *SAE AMS 2700F*; Passivation of Corrosion Resistant Steels. Aerospace Material Specification. SAE International: Warrendale, PA, USA, 2018.
34. *ASTM G44-99*; Standard Practice for Exposure of Metals and Alloys by Alternate Immersion in Neutral 3.5% Sodium Chloride Solution. ASTM International: West Conshohocken, PA, USA, 1999.
35. *ASTM G106-15*; Standard Practice for Verification of Algorithm and Equipment for Electrochemical Impedance Measurements. ASTM International: West Conshohocken, PA, USA, 2015.
36. Macdonald, D.D. The history of the Point Defect Model for the passive state: A brief review of film growth aspects. *Electrochim. Acta* **2011**, *56*, 1761–1772.
37. Duan, Z.; Man, C.; Dong, C.; Cui, Z.; Kong, D.; Wang, L.; Wang, X. Pitting behavior of SLM 316L stainless steel exposed to chloride environments with different aggressiveness: Pitting mechanism induced by gas pores. *Corros. Sci.* **2020**, *67*, 108520.
38. Choudhary, S.; Qiu, Y.; Thomas, S.; Birbilis, N. Element-resolved electrochemical analysis of transpassive dissolution and repassivation behavior of the multi-principal element alloy AlTiVCr. *Electrochim. Acta* **2020**, *362*, 137104. [[CrossRef](#)]
39. Tian, H.; Sun, F.; Chu, F.; Wang, L.; Wang, X.; Cui, X. Passivation behavior and surface chemistry of 316 SS in the environment containing Cl⁻ and NH₄⁺. *J. Electroanal. Chem.* **2021**, *886*, 115138.
40. Samaniego-Gámez, P.; Almeraya-Calderón, F.; Martin, U.; Ress, R.; Gaona-Tiburcio, C.; Silva-Vidaurre, J.; Cabral-Miramontes, J.; Bastidas, J.; Chacón-Nava, J.; Bastidas, M.D. Effect of sealing treatment on the corrosion behavior of anodized AA2099 aluminum-lithium alloy. *Rev. Metal.* **2020**, *56*, e180. [[CrossRef](#)]
41. Blanco, G.; Bautista, A.; Takenouti, H. EIS Study of Passivation of Austenitic and Duplex Stainless Steels Reinforcements in Simulated Pore Solutions. *Cem. Concr. Compos.* **2006**, *28*, 212–219. [[CrossRef](#)]
42. Warren, J.; Wei, D.Y. The low cycle fatigue behavior of the controlled transformation stainless steel alloy AM355 at 121, 204 and 315 °C. *Mater. Sci. Eng. A* **2008**, *475*, 148–156. [[CrossRef](#)]
43. Tseng, K.H.; Chen, Y.C.; Chen, Y.C. Micro Plasma Arc Welding of AM 350 Precipitation Hardening Alloys. *Appl. Mech. Mater.* **2012**, *121*, 2681–2685. [[CrossRef](#)]
44. Favor, R.J.; Deel, O.L.; Achbach, W.P. *Design Information on AM-350 Stainless Steel for Aircraft and Missiles*; Defense Metals Information Center, Battelle Memorial Institute: Columbus, OH, USA, 1961; Volume 156.
45. Grubać, Z.; Metikoš-Huković, M. EIS Study of Solid-State Transformations in the Passivation Process of Bismuth in Sulfide Solution. *J. Electroanal. Chem.* **2004**, *565*, 85–94. [[CrossRef](#)]
46. Shaikh, H.; George, G.; Khatak, H.S. Failure analysis of an AM 350 steel bellows. *Fail. Anal.* **2001**, *8*, 571–576. [[CrossRef](#)]
47. Lin, C.K.; Chu, C.C. Mean stress effects on low-cycle fatigue for a precipitation-hardening martensitic stainless steel in different tempers. *Fatigue Fract. Eng. Mater. Struct.* **2000**, *23*, 545–553. [[CrossRef](#)]
48. Boudinar, Y.; Belmokre, K.; Touzet, M.; Devos, O.; Puiggali, M. Investigation of the Passivation Process of Plastically Deformed 316L Stainless Steel Using the High Frequency Capacitance Obtained by EIS. *Mater. Corros.* **2019**, *70*, 206–215. [[CrossRef](#)]
49. Freire, L.; Carmezim, M.J.; Ferreira, M.G.S.; Montemor, M.F. The Electrochemical Behaviour of Stainless Steel AISI 304 in Alkaline Solutions with Different PH in the Presence of Chlorides. *Electrochim. Acta* **2011**, *56*, 5280–5289. [[CrossRef](#)]
50. Recio-Hernandez, J.; Galicia-García, M.; Silva-Jiménez, H.; Malpica-Calderón, R.; Ordoñez-Casanova, E.G. EIS Evaluation of Corrosion Resistance of AISI 304 Stainless Steel Exposed to Pseudomonas Stutzeri. *Int. J. Electrochem. Sci.* **2021**, *16*, 21058. [[CrossRef](#)]
51. Olugbade, T.O.; Omiyale, B.O. Corrosion Study and Surface Analysis of the Passivation Film on Surface-Deformed AISI 304 Stainless Steel. *Chem. Afr.* **2022**, *5*, 1663–1670. [[CrossRef](#)]
52. Zhang, H.; Zhao, J.; Yang, C.; Shen, M.; Zhang, X.; Xi, T.; Yin, L.; Zhao, H.; Liu, X.; Liu, L.; et al. Corrosion Resistance of Cu-Bearing 316L Stainless Steel Tuned by Various Passivation Potentials. *Surf. Interface Anal.* **2021**, *53*, 592–602. [[CrossRef](#)]
53. Chokri, A.; Ben Rhouma, A.; Sahlaoui, H. *Evaluation of Passivation and Corrosion Behavior of AISI 316L SS with Low Ferrite Content Using EIS Test in Artificial Seawater Solution*; Lecture Notes in Mechanical Engineering; Springer: Cham, Switzerland, 2024; pp. 19–28. [[CrossRef](#)]
54. Cheng, X.; Li, X.; Yang, L.; Du, C. Corrosion Resistance of 316L Stainless Steel in Acetic Acid by EIS and Mott-Schottky. *J. Wuhan Univ. Technol. Mater. Sci. Ed.* **2008**, *23*, 574–578. [[CrossRef](#)]

55. Niu, W.; Lillard, R.S.; Li, Z.; Ernst, F. Properties of the Passive Film Formed on Interstitially Hardened AISI 316L Stainless Steel. *Electrochim. Acta* **2015**, *176*, 410–419. [[CrossRef](#)]
56. Kang, J.; Li, J.; Zhao, K.Y.; Bai, X.; Yong, Q.L.; Su, J. Passivation Behaviors of Super Martensitic Stainless Steel in Weak Acidic and Weak Alkaline NaCl Solutions. *J. Iron Steel Res. Int.* **2015**, *22*, 1156–1163. [[CrossRef](#)]
57. Lai, W.Y.; Zhao, W.Z.; Yin, Z.F.; Zhang, J. EIS and XPS Studies on Passive Film of AISI 304 Stainless Steel in Dilute Sulfuric Acid Solution. *Surf. Interface Anal.* **2012**, *44*, 418–425. [[CrossRef](#)]
58. Wallinder, D.; Pan, J.; Leygraf, C.; Delblanc-Bauer, A. EIS and XPS Study of Surface Modification of 316LVM Stainless Steel after Passivation. *Corros. Sci.* **1998**, *41*, 275–289. [[CrossRef](#)]
59. Alves, V.A.; Brett, C.M.A. Characterisation of Passive Films Formed on Mild Steels in Bicarbonate Solution by EIS. *Electrochim. Acta* **2002**, *47*, 2081–2091. [[CrossRef](#)]
60. Cabrera-Sierra, R.; Hallen, J.M.; Vazquez-Arenas, J.; Vázquez, G.; González, I. EIS characterization of tantalum and niobium oxide films based on a modification of the point defect model. *J. Electroanal. Chem.* **2010**, *638*, 51–58. [[CrossRef](#)]
61. Chávez-Díaz, M.P.; Luna-Sánchez, R.M.; Vazquez-Arenas, J.; Lartundo-Rojas, L.; Hallen, J.M.; Cabrera-Sierra, R. XPS and EIS Studies to Account for the Passive Behavior of the Alloy Ti-6Al-4V in Hank's Solution. *J. Solid State Electrochem.* **2019**, *23*, 3187–3196. [[CrossRef](#)]
62. Magar, H.S.; Hassan, R.Y.A.; Mulchandani, A. Electrochemical Impedance Spectroscopy (EIS): Principles, Construction, and Biosensing Applications. *Sensors* **2021**, *21*, 6578. [[CrossRef](#)]
63. Macdonald, J.R. Generalizations of “universal dielectric response” and a general distribution-of-activation-energies model for dielectric and conductive systems. *J. App. Phys.* **1985**, *58*, 1971–1978. [[CrossRef](#)]
64. Macdonald, J.R. Frequency response of inifield dielectric and conductive systems involving an exponential distribution of activation energy. *J. Appl. Phys.* **1985**, *58*, 1955–1970. [[CrossRef](#)]

Disclaimer/Publisher's Note: The statements, opinions and data contained in all publications are solely those of the individual author(s) and contributor(s) and not of MDPI and/or the editor(s). MDPI and/or the editor(s) disclaim responsibility for any injury to people or property resulting from any ideas, methods, instructions or products referred to in the content.